Supplementary Information

Synthesis of Fe_3O_4@C core–shell nanorings and their enhanced electrochemical performance for lithium-ion batteries

Lili Wang,[a] Jianwen Liang,[a] Yongchun Zhu,*[a] Tao Mei,[a] Xing Zhang,[a] Qing Yang[a] and Yitai Qian[a,b]

[a] *Hefei National Laboratory for Physical Science at Micro-scale, Department of Chemistry, University of Science and Technology of China*
Hefei, Anhui 230026, (P. R. China)；E-mail: ychzhu@ustc.edu.cn；Tel: +86-551-63601589
[b]*School of Chemistry and Chemical Engineering, Shandong University,*
Jinan, 250100, (P. R. China); E-mail: ytqian@ustc.edu.cn; Tel: +86-551-3607234

Experimental section

Synthesis of Fe_2O_3 precursors : All chemicals were of analytical grade and were purchased from Shanghai Chemical Industrial Corp. and used without further purification. The α-Fe_2O_3 nanorings were prepared by a modified hydrothermal method.[25] In a typical experimental procedure, specific amounts of $Fe(NO_3)_3$, $NH_4H_2PO_4$, and Na_2SO_4 aqueous solutions were mixed together, and then distilled water was added to the mixture to keep the final volume at 45 mL; the concentrations of $Fe(NO_3)_3$, $NH_4H_2PO_4$, and Na_2SO_4 were 0.02, 8.4×10^{-4}, and 5.5×10^{-4} mol L^{-1}, respectively. After 10 min stirring, the mixture was transferred into a Teflon-lined stainless steel autoclave with a capacity of 60 mL for hydrothermal treatment at 220 °C for 48 h. As the autoclave cooled down to room temperature, the red precipitate was harvested by centrifugation and washed with deionized water and absolute ethanol, and dried under vacuum at 60 °C overnight. Fe_2O_3 nanoerythrocytes was generated in the same way except a change in concentration of the reactants, and the concentrations of $Fe(NO_3)_3$, $NH_4H_2PO_4$ were 0.02 and 7.2×10^{-4}, respectively. No Na_2SO_4 was added.

Synthesis of R-Fe_3O_4@C : R-Fe_3O_4@C were prepared by thermal annealing acetylene with the precursor of R-Fe_2O_3. Typically, the dried α-Fe_2O_3 precursors were annealed in a furnace at 420 °C under a continuous acetylene/argon gas flow [C_2H_2/Ar=1/9] at a constant rate of 6 mL/ min for 10 h, followed by natural cooling to room temperature. A black powder was then collected and stored in a clean glass bottle for

later characterization.

Characterization: Products were characterized using XRD (Philips X'pert PRO X-ray diffractometer, Cu Kα, 1.54182 Å), SEM (JEOL-JSM-6700F), TEM (Hitachi H7650), HRTEM and SAED (JEOL 2010), XPS (VGESCA-LAB MKII). Raman spectrum was tested on a JYLABRAM-HR Confocal Laser Micro-Raman spectrometer with 514.5 nm from an argon laser at room temperature. EA (Elementar vario EL cube, Thermal Conductivity Detector) was used to determine the precise carbon content in composites. Thermogravimetric analysis (TGA) was measured from room temperature to 700 °C in air with a heating rate of 10 °C min^{-1}.

Electrochemical measurements: The electrochemical performance versus Li was tested using coin-type 2016 cells. To prepare the working electrodes, 60 wt% active materials, 25 wt% of carbon black, and 15 wt % of sodium carboxymethyl cellulose (CMC) as the binder were mixed homogeneously with deionized water. The obtained slurry was then pasted on Cu foil and dried at 120 ºC for 12 h in vacuum. The coin cells were assembled in an argon-filled glove box (Celgard 2400) with Li metal as an anode, and with the solution of 1.0 M LiPF6 in ethylene carbonate (EC)/diethyl carbonate (DEC) (1:1 by volume) as the electrolyte. The galvanostatic discharge/charge tests were conducted on a battery cycler (Land-CT2001A) in the voltage range of 0.01–3.0 V (vs. Li^+/Li) at room temperature. EIS were performed on CHI660D electrochemical workstation. The electrode after cycling was disassembled from the coin cell, and soaked into dimethyl carbonate (DMC) for 24 h, then washed with ethanol to remove the residual electrolyte, followed by drying under vacuumat 80 °C overnight. The sample now was ready for further SEM imaging.[20]

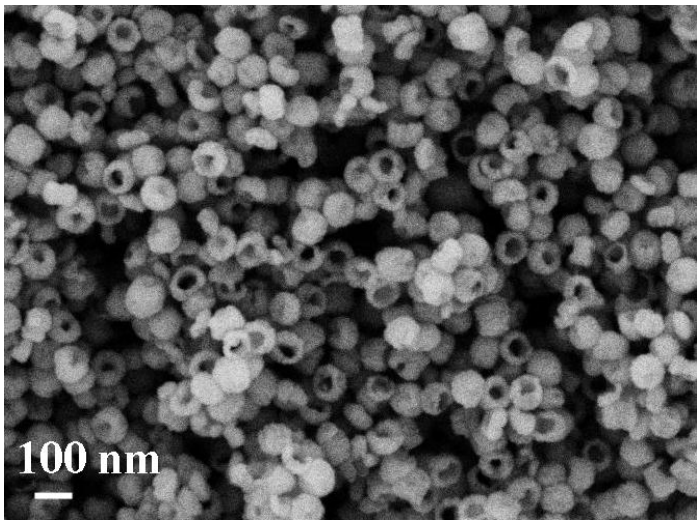

Figure S1 SEM images of R-Fe_2O_3.

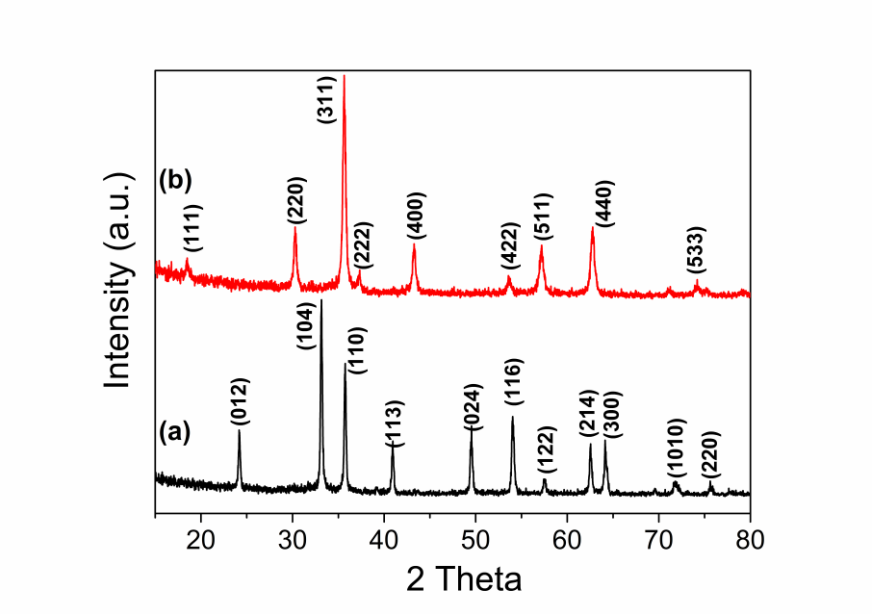

Figure S2 The XRD pattern of R-Fe_2O_3 (a) and R-Fe_3O_4@C (b).

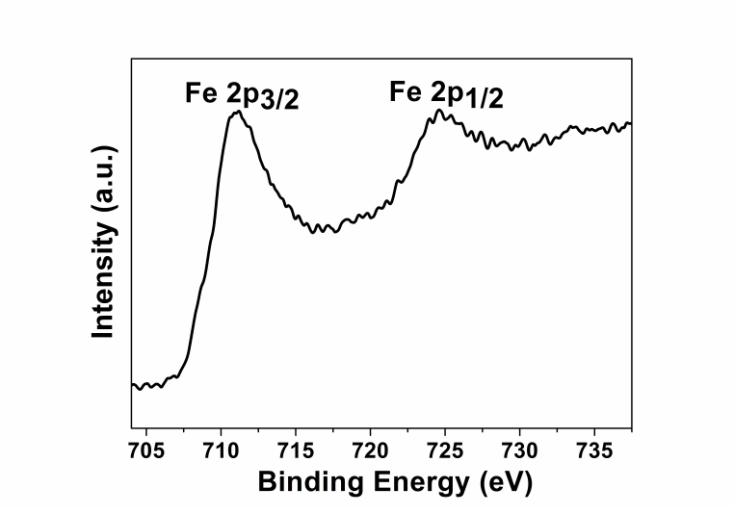

Figure S3 Fe 2p core-level spectra of the R-Fe_3O_4@C.

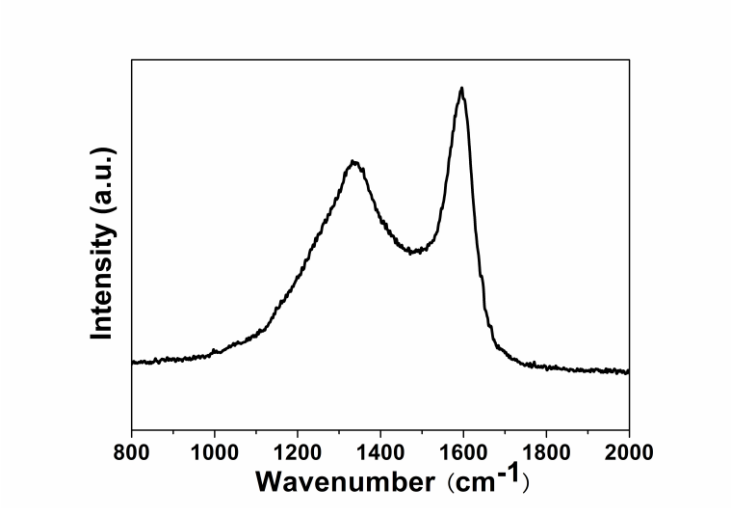

Figure S4 Raman spectrum of the R-Fe_3O_4@C.

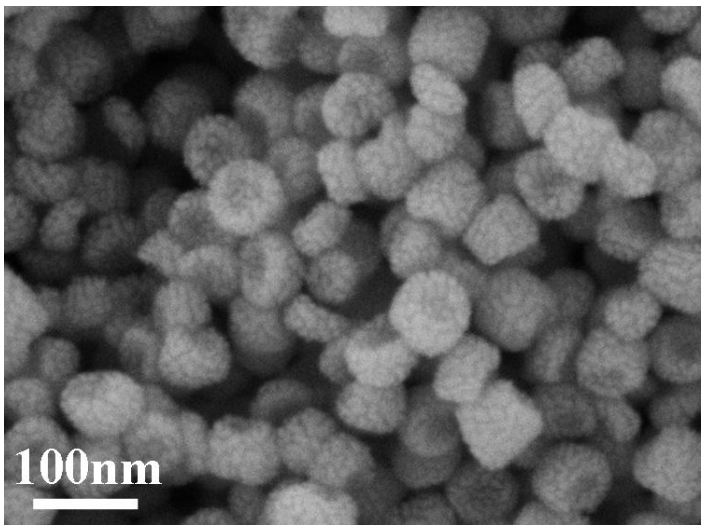

Figure S5 SEM images of E-Fe_2O_3.

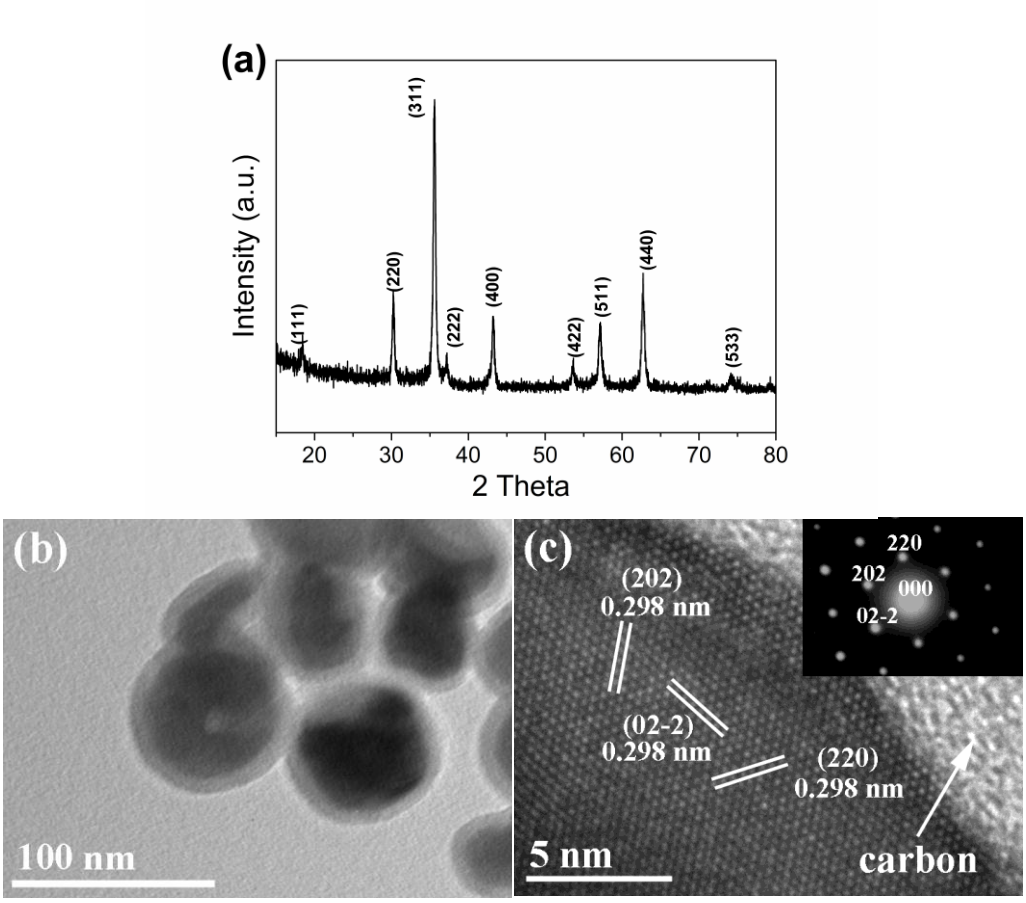

Figure S6 (a) The XRD pattern of E-Fe_2O_3 (b) TEM images and (c) HRTEM images and (insets) SAED patterns of E-Fe_3O_4@C.

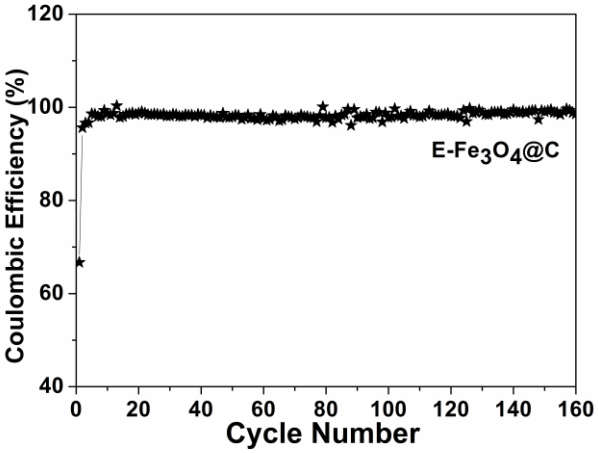

Figure S7 Coulombic efficiency of E-Fe_3O_4@C at a current density of 200 mA g^{-1}.

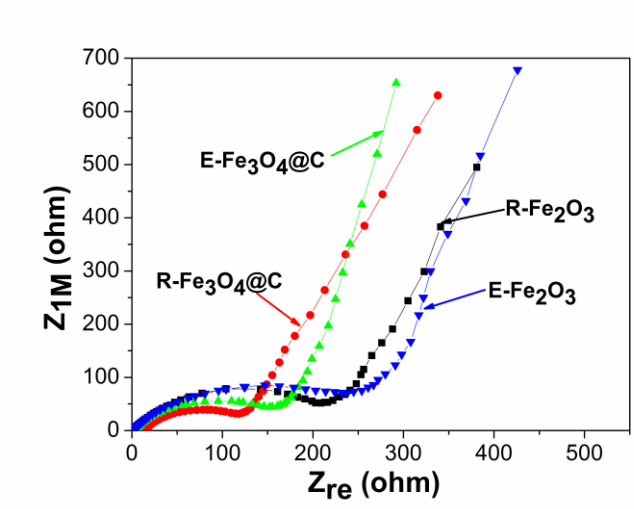

Figure S8 AC impedance of the electrodes composed of R-Fe_3O_4@C, E-Fe_3O_4@C, R-Fe_2O_3, and R-Fe_2O_3.

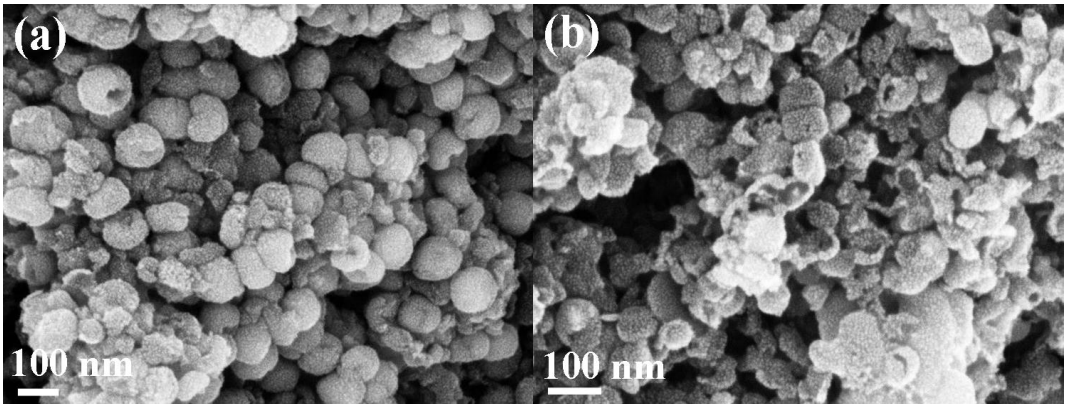

Figure S9 SEM images of (a) R-Fe_3O_4@C electrode and (b) E-Fe_3O_4@C after 70 cycles at diverse high rate from 100 to 1000 mA g^{-1}.

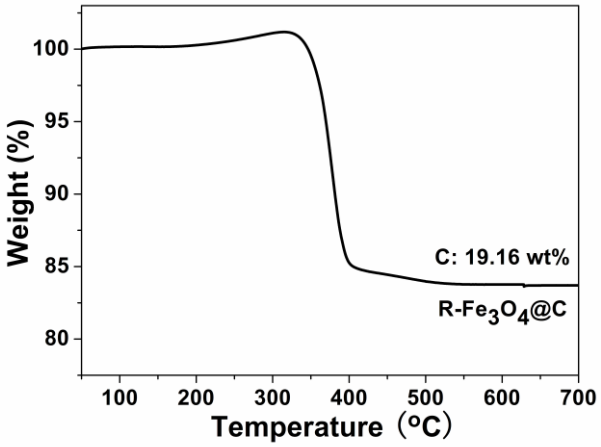

Figure S10 TG curves of R-Fe_3O_4@C.

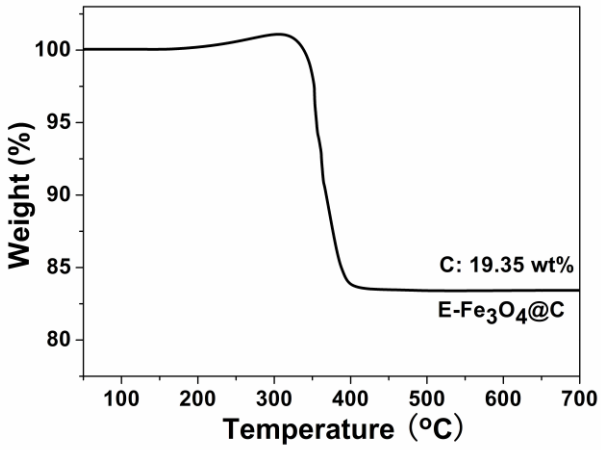

Figure S11 TG curves of E-Fe_3O_4@C.

Table S1 Comparison between the R-Fe_3O_4@C and previously reported Fe_3O_4@C structures

Material	Reversible capacity/mAh g^{-1}	Rate (mA g^{-1})	Initial efficiency	Ref.
Fe_3O_4@C core-shell nanorings	923/160th cycles	200	70.6%	This work
Fe_3O_4@C nanorods	808.2/100th cycles	924	67%	[14]
Fe_3O_4@C nanorods	394/100th cycles	100	71.7%	[15]
Fe_3O_4/carbon nanotubes	656/145th cycles	100	67%	[16]
Fe_3O_4/C composites	~630/100th cycles	184.8	--	[17]
Fe_3O_4/mesocellular carbon foam	~930/130th cycles	500	59%	[18]
Hollow Fe_3O_4/C spheres	984/70th cycles	200	68.6%	[19]
Fe_3O_4/C nanospindles	530/80th cycles	462	80%	[20]
Fe_3O_4/C nanoparticles	809/100th cycles	500	52%	[21]
Fe_3O_4@C core-shell spheres	782/100th cycles	184.8	--	[22]